

APPENDIX A

Final Report by University of Pittsburgh

Attrition Resistant Iron-Based Fischer-Tropsch Catalysts

FINAL REPORT

Work Performed Under
Grant No. DE-FG22-96PC96217

For
U.S. Department of Energy
Federal Energy Technology Center
Pittsburgh, PA 15236

By
Rong Zhao
James G. Goodwin, Jr.
Department of Chemical and Petroleum Engineering
University of Pittsburgh
Pittsburgh, PA 15260

October 1999

DISCLAIMER

This report was prepared as an account of work sponsored by an agency of the United States Government. Neither the United States Government nor any agency thereof, nor any of their employees, makes any warranty, express or implied, or assumes any legal liability or responsibility for the accuracy, completeness, or usefulness of any information, apparatus, product, or process disclosed, or represents that its use would not infringe privately owned rights. Reference herein to any specific commercial product, process, or service by trade name, trademark, manufacturer, or otherwise, does not necessarily constitute or imply its endorsement, recommendation, or favoring by the United States Government or any agency thereof. The views and opinions of authors expressed herein do not necessarily state or reflect those of the United States Government or any agency thereof.

ABSTRACT

Fischer-Tropsch Synthesis (FTS) is one of the major indirect routes for converting syngas ($\text{CO}+\text{H}_2$). Iron Catalysts are the preferred catalysts for the conversion of syngas based on coal, due to their water gas (WGS) capabilities. Since FTS is highly exothermic, slurry bubble column reactors (SBCRs) has been suggested for this reaction due to their excellent heat removal capability. However, the catalyst attrition encountered, especially when iron catalyst is used, has hindered the application of SBCRs. To improve the physical strength of the iron catalysts, the spray drying technique has recently been used for preparation of iron SBCR Fischer-Tropsch (F-T) catalysts. However, the effects of such preparation in the improvement of catalyst attrition resistance are still not clear.

In this study, two series of spray dried iron F-T catalysts having the composition Fe/Cu/K/SiO₂ have been studied to better understand the characteristics important for attrition resistance. XRD results confirmed that the catalysts after calcination are in the same hematite Fe₂O₃ phase. Crystallinity and BET surface area were found not to be relevant to the catalyst attrition performance. TPR results indicated little or no SiO₂ and metal interaction. However, the porosity of the catalysts was found to be relevant to the catalyst attrition resistance. After acid leaching of the catalysts, further study of the SiO₂ in the catalyst showed a porous and uniform SiO₂ construct is suggested to provide the best attrition resistance for the catalysts.

Since phase change during reaction has always been a concern for iron catalysts in terms of attrition resistance, some of the catalysts were carburized and tested using the jet cup. The attrition resistance was found to actually improve after carburization.

ACKNOWLEDGMENTS

This study was sponsored by the U.S. Department of Energy (DOE) under Grant No: DE-FG-22-96PC96217. The authors would like to acknowledge with gratitude the guidance provided by the DOE Contracting Officer's Representative, Dr. Richard E. Tischer.

CONTENTS

<u>Section</u>		<u>Page</u>
	Abstract	33
	Acknowledgments	34
1.0	Introduction	36
2.0	Experiments	37
2.1	Catalyst Preparation.....	37
3.0	Catalyst Characterization.....	38
3.1	Attrition Resistance.....	38
3.2	Particle Morphology.....	39
3.3	Particle Size Distribution.....	39
3.4	BET Surface Area and Pore Size Distribution	39
3.5	Reducibility.....	40
3.6	Phase and Crystallinity.....	40
4.0	Results	40
5.0	Discussion	54
6.0	Conclusion.....	63
7.0	References.....	65
	Appendix B. Attrition Assessment for SBCR Catalysts.....	66

1.0 INTRODUCTION

Fischer-Tropsch synthesis (FTS) is one of the major indirect ways of converting coal into a wide variety of hydrocarbons. Iron-based catalysts are the preferred catalysts for FTS based on coal and have been a research focus for FTS recently (Bukur et al., 1990; 1996; Schulz et al., 1994; Kalakkad et al., 1995; Huang et al., 1993). Such catalysts are relatively inexpensive, possess reasonable activity for FTS, and have high WGS activity compared to cobalt catalysts. This enables iron Fischer-Tropsch (F-T) catalysts to process low H_2/CO ratio syngas without an external shift reaction step.

In the development of FTS over the past 20 years, the application of slurry bubble column reactors (SBCRs) has drawn much attention. This is due to their excellent heat removal capability of SBCRs during reaction. Since FTS is a highly exothermic reaction, the use of SBCRs can largely solve the reaction control problem. However, commercial application of SBCRs is just now being to be applied. One of the major drawbacks in the industrial application of SBCRs is catalyst attrition, especially when iron catalysts are used (Bhatt et al., 1997). The attrition of catalysts in SBCRs causes filter plugging problems as well as lower product quality. The use of supported iron catalysts can improve the catalyst attrition resistance, but at the expense of lower specific catalyst activity.

In order to try to improve the physical strength of the catalysts without sacrificing their activity, the spray drying technique has been recently used in the preparation of iron F-T catalysts (Srinivasan et al., 1996; Jothimurugesan et al., 1999). This improvement in physical strength by use of spray drying has stimulated much interest in preparing iron F-T catalysts by this technique as well. In practice, many parameters are relevant to final catalyst attrition resistance, such as solids concentration in the slurry, calcination temperature etc. Different preparation conditions result in different catalyst morphology, BET surface area, and porosity,

which can affect not only the catalyst attrition resistance, but also the catalyst activity. The effects of each preparation parameter on the performance of a catalyst are therefore complex.

In the present research, the structures of two series of spray-dried Fe catalysts were studied. The goal was to investigate the relationship between the structure of the catalysts and binder material and their attrition resistances. At the absence of iron phase change, such understanding can help us to better address the impact of the catalyst physical properties on catalyst strength and separate these phase effects from further studies of Fe catalyst attrition performance under reaction conditions. Preliminary results had indicated significant differences in attrition resistance and it was desired to better understand these differences. The effects of type and concentration of refractory silica (precipitated or binder silica), as well as morphology and porosity of particles on attrition resistance of spray dried iron catalysts are addressed.

2.0 EXPERIEMENTS

2.1. Catalyst Preparation

The iron catalysts were prepared at Hampton University and then it was shipped to University of Pittsburgh for attrition tests. In brief, two series of iron catalysts were prepared for this study. One series of catalysts were prepared without precipitated silica but with different weight percentages of binder silica. The other series of catalysts were prepared with different levels of precipitated silica and with 12 wt % of binder silica. For both series, catalysts were prepared having compositions of 100Fe/5Cu/4.2K/xSiO₂ by weight. First precipitation from an aqueous solution containing Fe(NO₃)₃·9H₂O, Cu(NO₃)₂·2.5H₂O, Si(OC₂H₅)₄ (if added to give precipitated SiO₂) in the desired ratio by the addition of ammonium hydroxide. This precipitate was then slurried with the binder SiO₂ precursor. The final step was to spray dry the catalysts at 250°C in a Niro Spray drier, which is scalable spray drier. After spray drying, the catalysts were

then calcined at 300°C for 5 hours in a muffle furnace. The detailed preparation conditions and procedures can be found in section 3.1 of the main text.

In this report, the following nomenclature is used: the letter **p** represents precipitated silica while the letter **b** stands for binder silica. For example, a catalyst designated as Fe-bSi(12) refers to an iron catalyst prepared without precipitated silica but with 12 wt % binder silica. Since the concentrations of Cu and K were not varied relative to Fe, they are not addressed in the nomenclature used. In addition, since two different types of SiO₂ was used in the preparation of catalysts, i.e. precipitated and binder SiO₂, the term SiO₂ study refers to either or both of them.

In order to study the precipitated and/or binder silica incorporated in the catalysts, acid leaching was performed by treating the catalysts using an HCl solution. After the iron dissolved, the SiO₂ remaining was washed 5 times using deionized water. After filtration, the SiO₂ was dried under vacuum condition at room temperature in order to avoid any possible agglomeration caused by heating.

3. CATALYST CHARACTERIZATION

3.1 Attrition Resistance

The attrition resistance of the catalysts were evaluated using the jet cup test, a proposed ASTM method and one which has been demonstrated to cause attrition characteristic in an SBCR (Zhao et al., 1999). In the present study, 5 grams of each sample were used for the attrition tests, which were all performed using the air flow rate of 15 l/min with a relative humidity of 60 % at room temperature for 1 hour. The detailed attrition assessment study for SBCR catalysts, system configuration and test procedure can be found in Appendix B. The fines were collected by a thimble filter at the outlet of the jet cup chamber and were analyzed for particle size distribution together with the particles remaining in the chamber.

3.2. Particle Morphology

Particle morphology was obtained for each catalyst (as prepared and after attrition testing) and acid-leached sample using a Philips XL30 FEG Scanning Electron Microscope (SEM). The samples were coated with palladium before measurement to avoid charging problems.

3.3. Particle size Distribution

A Leeds & Northrup Microtrac Model 7990-11 laser particle size analyzer was used in order to measure the particle size distributions. Both size distributions of the samples as prepared and after jet cup testing were measured. Each sample was put into 50 ml of deionized water and dispersed using an ultrasonic bath. The results of several measurements of the same sample averaged in order to minimize the error. The detailed sampling and measuring procedures were described in Appendix B.

Since size distribution in attrition studies are usually plotted as weight (or volume) percentage versus average projected area diameter of particles, change in the volume moment, a type of average particle size commonly used to represent a particular PSD, has been selected as a useful indicator of the attrition process. The volume moment, x_{VM} , can be calculated by (Allen, 1997).

$$x_{VM} = x_{WM} = \frac{\sum dM}{\sum dV} = \frac{\sum x^4 dN}{\sum x^3 dN} \quad (1)$$

where, x_{VM} is the volume moment, x_{WM} the weight moment, M the size moment, V the particle volume, and N the number of particles of size (diameter) x .

3.4. BET Surface Area and Pore Size Distribution

The BET surface area and pore size distribution (micropore and mesopore) of the catalysts were determined by N_2 physisorption using a Micromeritics ASAP 2010 automated

system. The samples were degassed in the Micromeritics ASAP 2010 at 100°C for 1 hour, and then 300°C for two hours prior to each measurement. These parameters were determined for both catalyst samples as prepared and after attrition tests.

3.5. Reducibility

The reducibility of the iron catalysts as prepared were measured by temperature programmed reduction (TPR) using an Altamira AMI-1 systems. The TPR measurements were carried out using 5% H₂ in Ar with a flow rate of 30 cc/min and the temperature was ranged from 30°C up to 900°C at a ramping rate of 5°C/min.

3.6. Phase and Crystallinity

X-ray powder diffraction patterns were obtained using a Philips PW1800 x-ray unit using Cu|K α radiation. Analysis was conducted for each catalyst sample as prepared and some samples after acid leaching using a continuous scan mode at a scan rate of 0.05° (2 θ) per second.

4.0 RESULTS

The attrition resistance results for all the iron catalysts studied are summarized in Table 1. It can be seen that catalysts without precipitated silica in general are relatively more attrition resistant compared to the catalysts with precipitated silica. For the series of catalysts with precipitated silica, the attrition resistance obviously decreased with an increase in the

Table 1. Jet cup attrition resistance test results of the spray dried iron catalysts.

Catalyst	Coprecipitated Silica (pbw)	Binder Silica (wt%)	Fines (wt%) ^(a)	Original Volume Moment (μm) ^(c)	Volume Moment after Test (μm) ^(c)	Net change in Volume Moment (%)
Fe-bSi(4)	0	4	26.6	78.0	39.2	49.7
Fe-bSi(8)	0	8	21.8	86.7	45.4	47.6
Fe-bSi(12)	0	12	8.5	88.8	67.8	23.6
Fe-bSi(16)	0	16	18.2	69.91	47.6	31.9
Fe-bSi(20)	0	20	51.6	63.5	23.7	62.7
Fe-pSi(5)	5	12	26.6	103.0	37.3	63.8
Fe-pSi(10)	10	12	33.9	83.0	34.1	58.9
Fe-pSi(15)	15	12	39.6	90.2	27.7	69.3
Fe-pSi(20)	20	12	41.3	85.9	30.1	65.0
Co/SiO ₂ ^(d)	N/A	N/A	31.07	79.88	45.16	43.47

(a) Fines wt% = weight of fines collected/weight of total catalyst recovered

(b) Weight increased = (total weight recovered / weight of loading) x 100% (due to the humidity of the air).

(c) Volume Moment is a volume mean diameter of the particles.

(d) Co035 is a Davison silica supported 20wt% cobalt catalyst, which was used for develop the procedure.

concentration of the precipitated silica. On the other hand, for the series of catalysts without precipitated silica, an optimum concentration of binder silica was observed in terms of improvement of the catalyst attrition resistance. The catalyst with 12 wt% of binder silica but no precipitated silica, Fe-bSi(12), appears to be the most attrition resistant one among all the catalysts tested. A cobalt catalyst with 20 wt% of cobalt prepared using incipient wetness of a spray dried silica is also listed in Table 1 as a benchmark. This cobalt catalyst was found to be suitable for use in an SBCR (Zhao et al., 1999). The comparison of the attrition results shows that some of the spray dried iron catalysts in their calcined state are physically as strong as, or stronger than, the cobalt catalysts. These iron catalysts are there for considered to have strong potential for SBCR use.

The XRD results of these catalysts verify that the components of the fresh catalysts are rather the same, consisting primarily of hematite Fe_2O_3 (Figure 1). A sample of hematite Fe_2O_3 (purity 99.98%), Aldrich Chemicals, Co., was also examined by XRD as a benchmark (see also Figure 1). Compared to this pure Fe_2O_3 sample, the iron catalysts was obviously less XRD crystalline. Other components, even the SiO_2 (binder silica and/or precipitated silica) were not detectable by XRD results for any of the catalysts.

The reducibility of the catalysts was determined using TPR and the results are listed in Table 2. The TPR results indicate that H_2 consumption during TPR decreased with an increase in the concentration of the binder silica. However, this change was due mainly to decrease in the overall concentration of iron oxide in the catalysts. The reducibilities of the iron catalysts were approximately the same (as an iron basis) for all the catalysts. In Figure 2, a typical reduction curve is shown. This curve is similar to other in the literature (Jothimurugesan et al., 1999). The first peak is considered to be the reduction of Fe_2O_3 to Fe_3O_4 and the second peak to be the

Figure 1. XRD results of the iron catalysts as prepared and Fe₂O₃ as benchmark

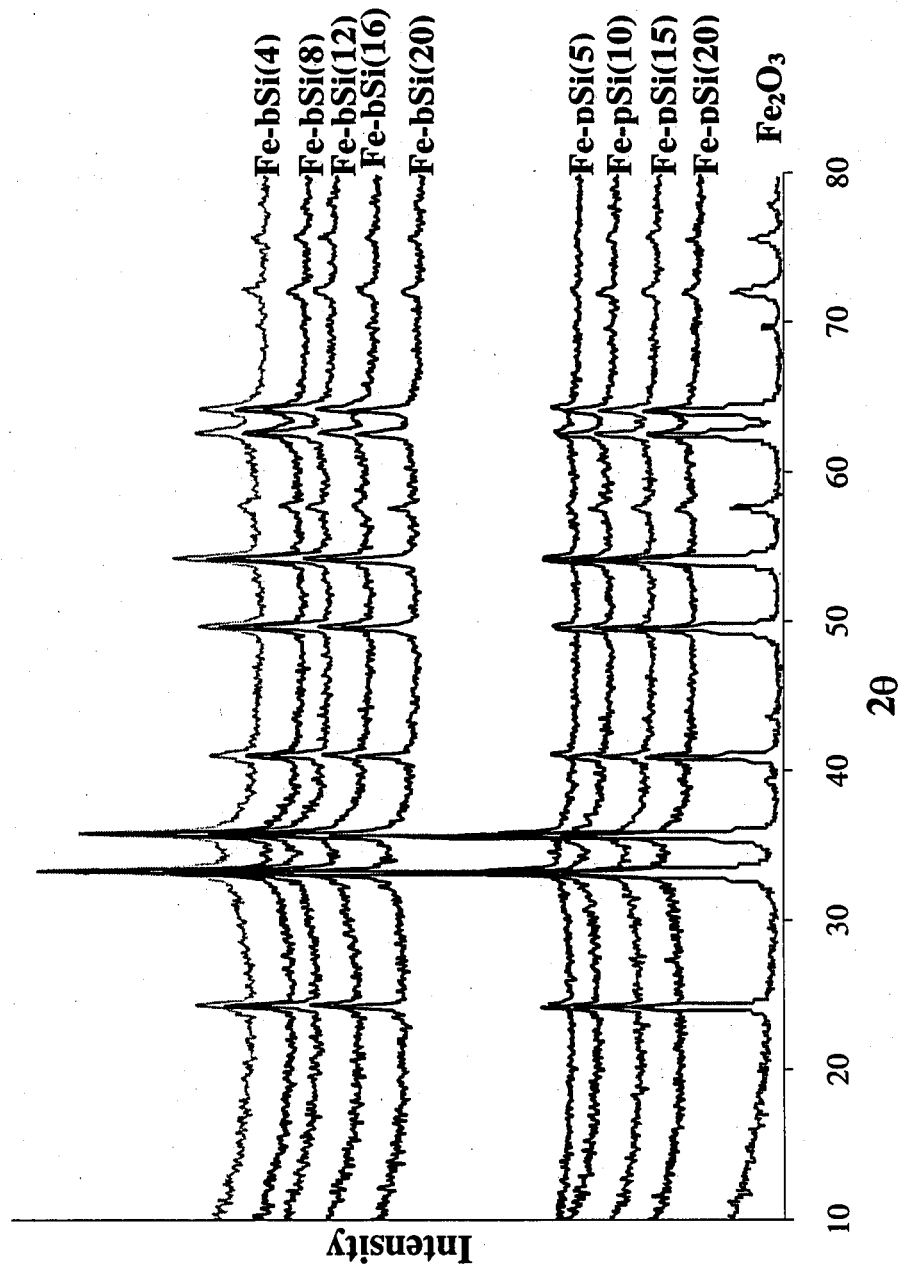
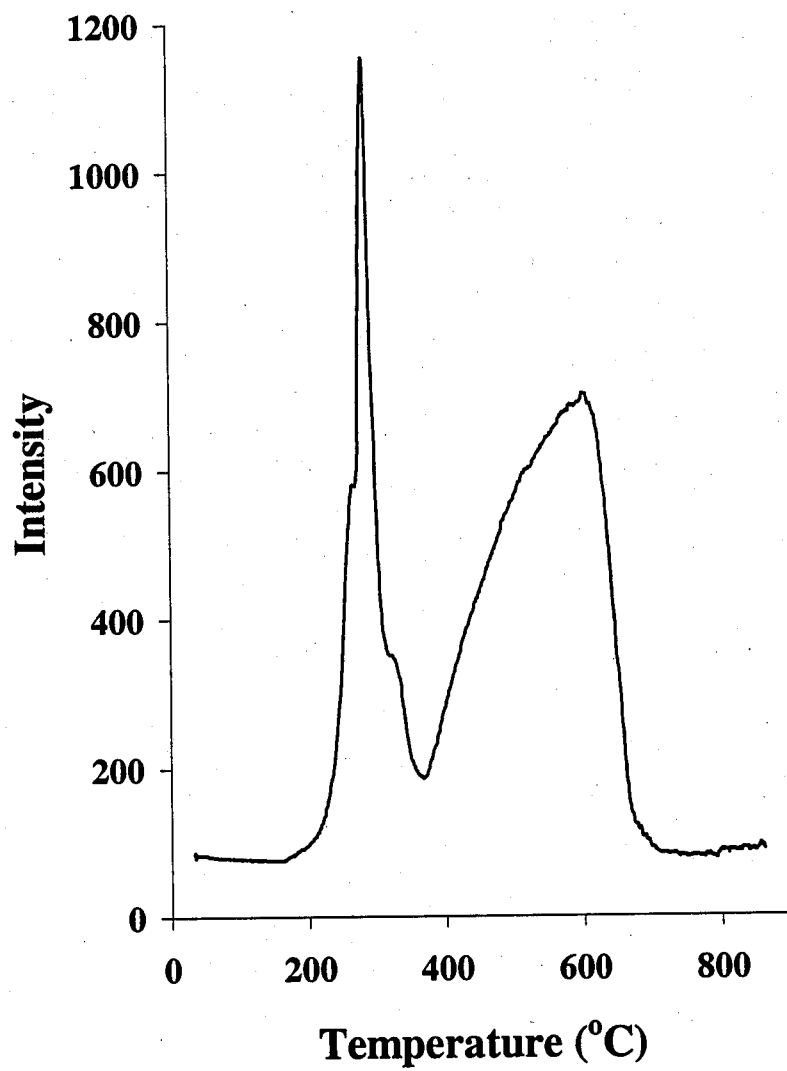


Table 2. TPR results of spray dried iron catalysts.

Catalyst	H₂ TPR (mmol H₂/g cat)	Reducibility (%)
Fe-bSi(4)	39.0	0.74
Fe-bSi(8)	38.8	0.76
Fe-bSi(12)	34.5	0.70
Fe-bSi(16)	34.9	0.74
Fe-bSi(20)	34.1	0.74
Fe-pSi(5)	34.6	0.74
Fe-pSi(10)	32.8	0.73
Fe-pSi(15)	33.1	0.77
Fe-pSi(20)	31.6	0.76

Figure 2. A typical TPR result [Fe-bSi(16) as prepared]



reduction of Fe_3O_4 to metallic iron. The small shoulder before the first peak has been suggested to be due to the reduction of the CuO .

The BET surface areas and average pore sizes were measured for both catalysts as prepared and after attrition tests using N_2 physisorption. As shown in Table 3, the BET surface areas, for each series of catalysts, generally increased with an increase in the concentration of SiO_2 . The series with precipitated silica had relatively higher surface areas compared to the series without precipitated silica. The pore volumes (micropore and mesopore) slightly increased with an increase in the concentration of SiO_2 . The series of catalysts with precipitated silica appears to have had higher pore volumes compare to the series without precipitated silica. The average pore sizes (calculated using $2 \times \text{pore volume} / \text{surface area}$) varied slightly for all the catalysts. In general there was a decrease in average pore size for both series of catalysts, as SiO_2 content increased-related obviously to the large increase in BET surface area. After the jet cup tests, the average pore sizes remained unchanged for all the catalysts compared to those of the catalysts as prepared, while the BET surface areas slightly decreased after the test for most catalysts.

Figure 3 and Figure 4 illustrate the morphologies of the catalyst with and without precipitated silica, respectively. For each catalyst, micrographs of the particles both as prepared and after attrition testing are shown. It is apparent that the particles were more spherical (less agglomeration) with the increase of binder concentration for both series of catalysts. There are relatively less agglomeration observed for the series of catalysts with precipitated silica and some "donut"-shape particles (the particles with holes) can be observed (where the arrows pointed in Figure 3). Such "donut"-shape particles are not observed for the series of catalysts without precipitated silica, even for those having higher concentration of binder silica.

Table 3. BET surface areas and average pore sizes of the iron catalysts.

Catalyst	BET Surface Area (m ² /g)		Pore Volume (cm ³ /g)		Average Pore Radius (Å)	
	Fresh	Attrited	Fresh	Attrited	Fresh	Attrited
Fe-bSi(4)	101.3	94.23	0.29	0.28	43.6	44.7
Fe-bSi(8)	124.6	108.1	0.28	0.26	35.3	36.1
Fe-bSi(12)	146.2	137.1	0.28	0.29	32.0	33.9
Fe-bSi(16)	176.6	173.1	0.37	0.34	33.8	33.3
Fe-bSi(20)	158.3	168.2	0.33	0.34	37.3	37.7
Fe-pSi(5)	179.4	180.5	0.34	0.34	35.2	35.8
Fe-pSi(10)	190.8	177.1	0.37	0.35	36.9	37.3
Fe-pSi(15)	216.8	188.7	0.36	0.33	30.8	33.4
Fe-pSi(20)	245.0	243.9	0.39	0.40	30.2	32.6

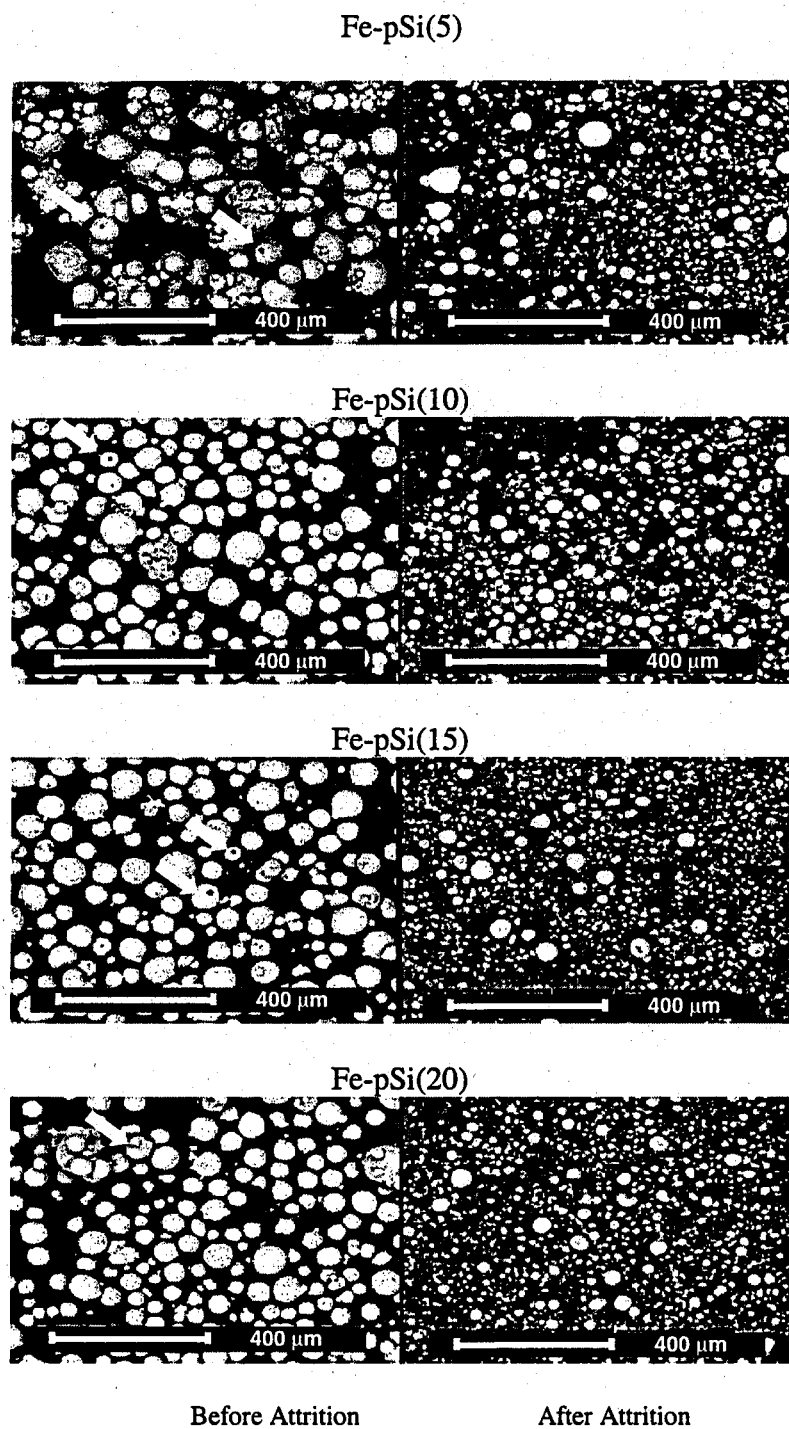
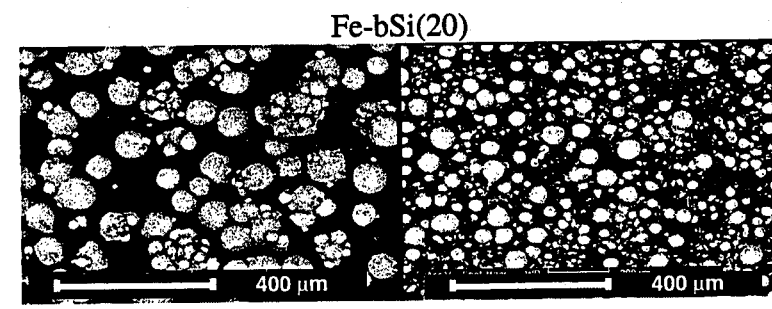
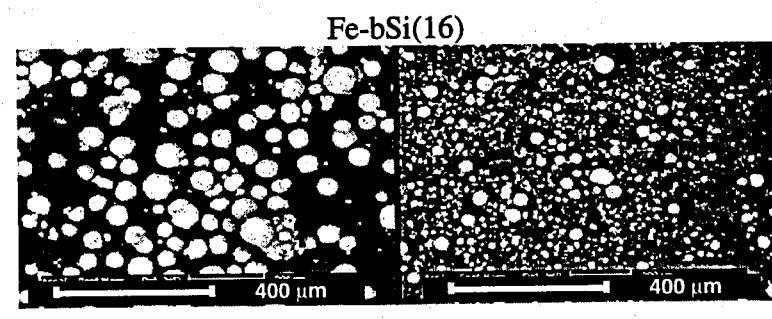
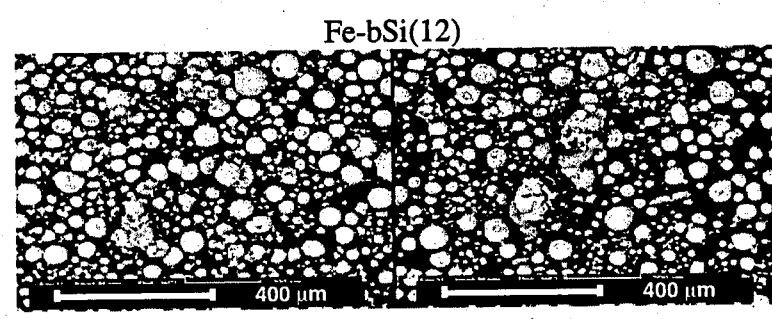
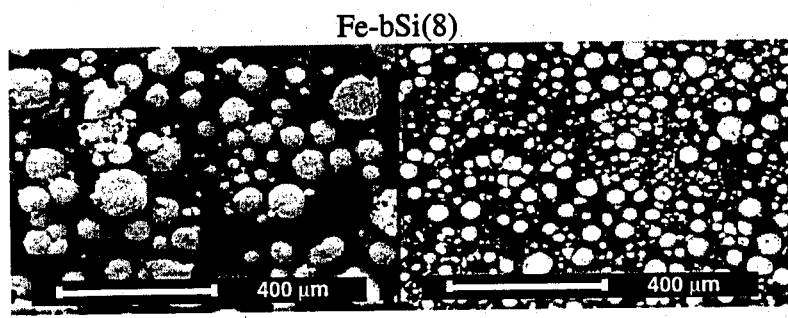
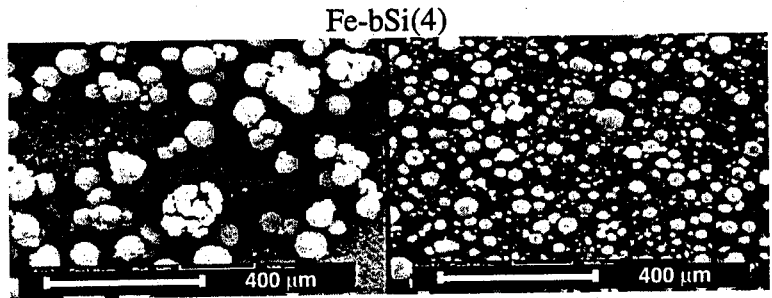


Figure 3. Morphology of the series of iron catalysts with precipitated silica



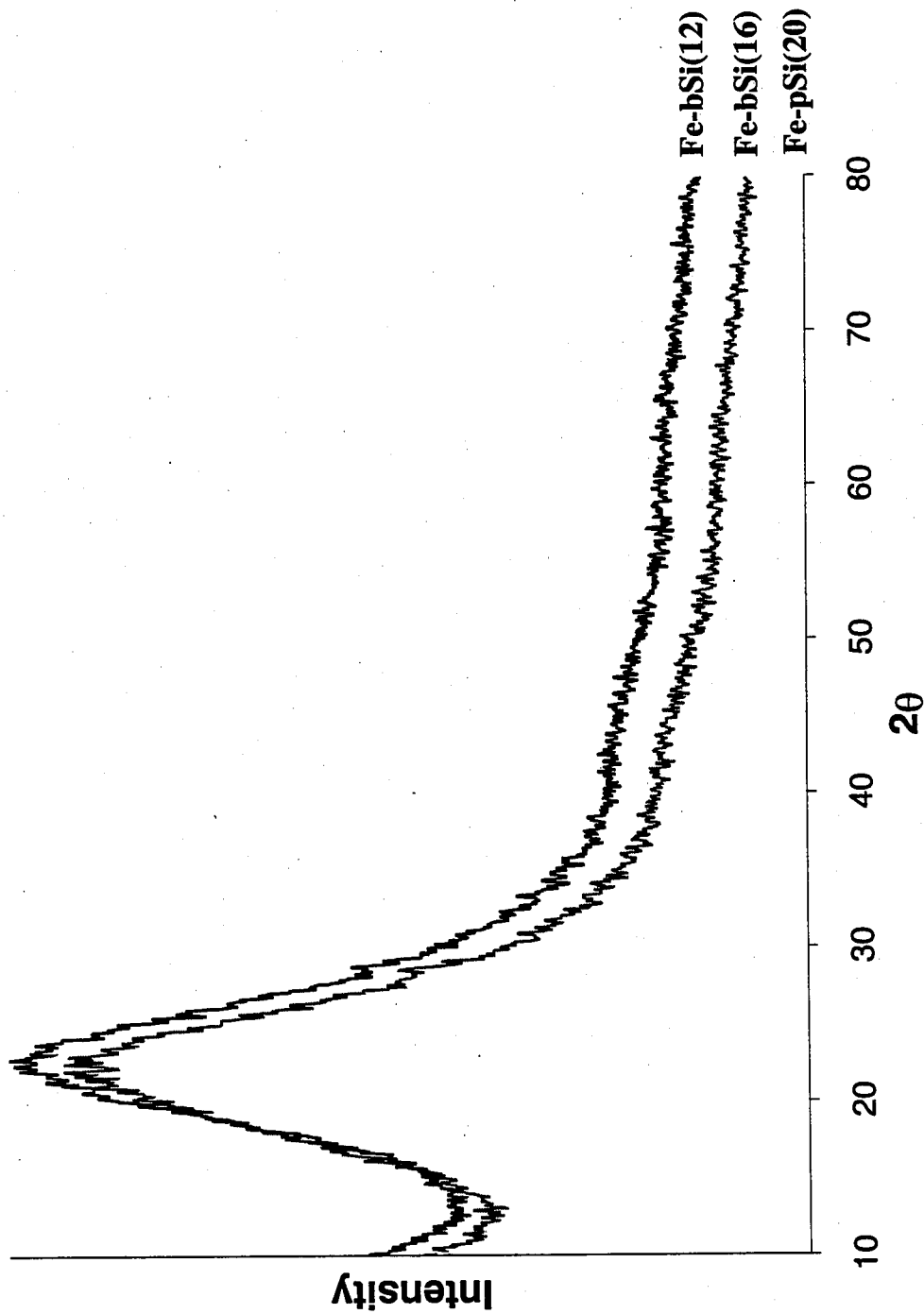
Before Attrition After Attrition
Figure 5. Morphology of binder silica catalysts.

When comparing the particles before and after attrition, it appears that the agglomerates formed during catalyst preparation were broken apart during the attrition test (Figures 3 and 4). The particle size obviously decreased for most catalysts after the attrition tests, especially for the series of catalysts with precipitated silica. The apparent decrease in the particle sizes was similar as seen by SEM and determined using laser diffraction. The only catalyst that did not change much in particle size was Fe-bSi(12), as also seen by particle size analysis. For this catalyst, some agglomerates still remained even after the jet cup test.

In order to study the phase and morphology of the supports, which plays an important role in attrition resistance of the catalysts, both series of catalysts were treated using acid leaching. This is due to the strong signal of iron oxide during XRD or SEM measures make the analysis of the supports very difficult. The XRD results of the supports are shown in Figure 5. The single peak in the XRD patterns shows that iron oxide is almost completely resolved during acid leaching. The supports are identified as silica, but are found all to be not crystallized.

The morphology of the supports was further studied using SEM. The results are summarized in Figure 6 and 7 for the supports of the series of catalysts with or without precipitated silica, respectively. The supports for the catalysts without precipitated silica (Figure 7) agglomerated more after dry compared to those without precipitated silica (Figure 6). The supports of the catalyst Fe-bSi(12) seem to agglomerate the least in series of catalyst without precipitated silica. On the contrary, the supports of the series of catalysts with precipitated silica seem to form individual spherical particle with very seldom agglomeration. There are also "donut"-shape particles that can be observed for the supports of the series of catalysts with precipitated silica (where the arrows pointed at in Figure 6).

Figure 5. XRD results of some of the silica supports of the iron catalysts



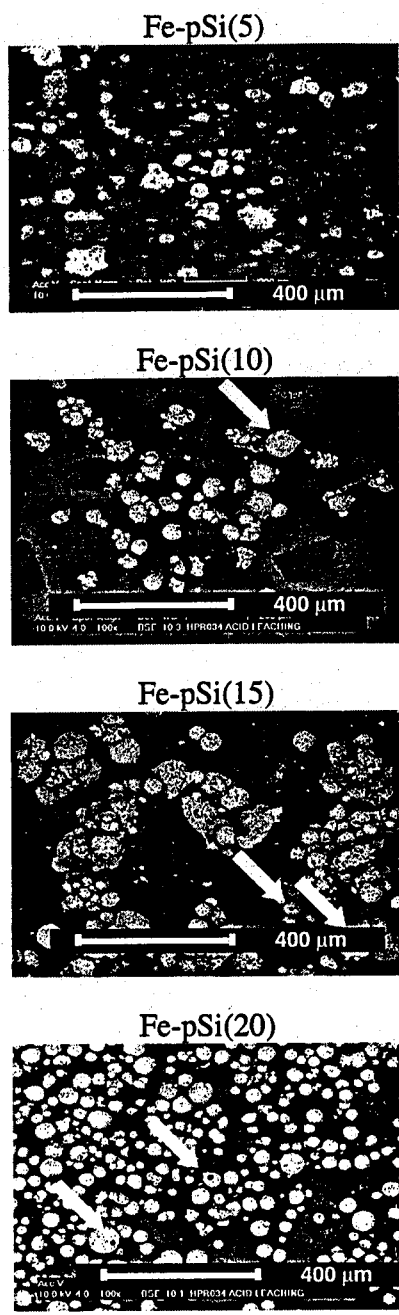
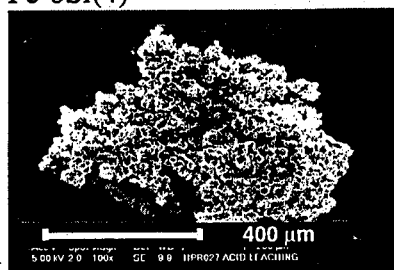
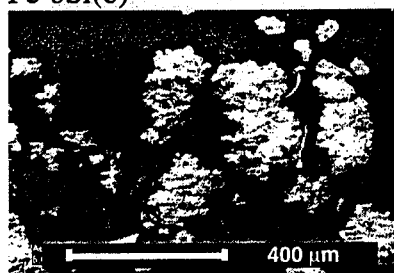


Figure 6. Morphology of the supports of the series of iron catalysts with precipitated silica

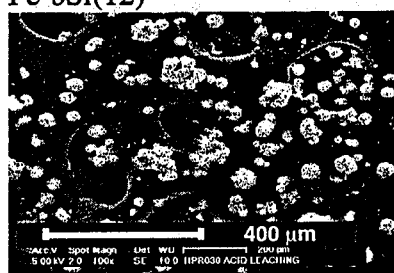
Fe-bSi(4)



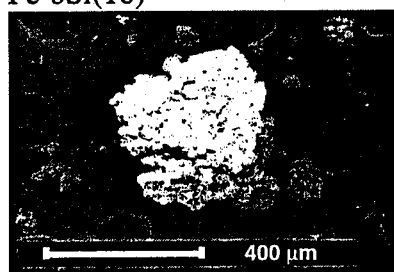
Fe-bSi(8)



Fe-bSi(12)



Fe-bSi(16)



Fe-bSi(20)

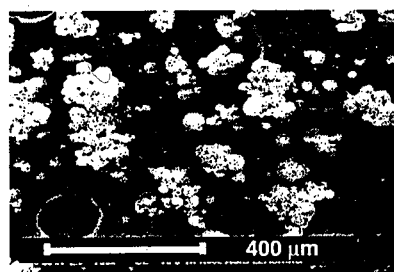


Figure 7. Morphology of the supports of the series of iron catalysts with binder silica

5.0 Discussion

Although the catalysts tested were prepared under similar conditions using spray dry technique, the attrition resistances vary in a large range (Table 1). After the addition of the precipitated silica, not only is the overall catalyst attrition resistance worse than that of the catalysts without precipitated silica, but also the attrition resistance decreases with the increase in the concentration of precipitated silica. Without the addition of the precipitated silica, it is not very clear how catalyst attrition resistance is affected by the concentration of the binder silica, even though there seems to be a trend of an optimum concentration of binder silica at ca. 12 wt %. In order to find out why and how the type and concentration of the supports have such an effect on attrition resistance, some further studies were performed.

As we expected, the XRD results (Figure 1) shows that the iron phase present in all the catalysts after calcination is Fe_2O_3 . It is less likely that the difference in attrition resistance was due to any phase difference. Nor is the crystallinity of the iron oxide found to be responsible for the differences in the catalyst attrition resistance. It is shown in Figure 1 that iron oxide in the catalysts are not as crystal as the pure Fe_2O_3 elements, but slight differences were found for all the catalysts.

To find out any possible support and metal interaction, the TPR analysis was carried out. The calculated results (Table 2) showed that the reducibilities of the catalysts are very close. The addition of precipitated silica does not appear to affect the catalyst reducibility. These results suggest an unlike interaction of the supports and iron metal.

It is apparent from the XRD and TPR results that the catalysts as prepared are not very different chemically, except for the concentrations of the components. Therefore, the physical properties of these catalysts have drawn more attention in our studies. The morphology of the

catalysts was determined using SEM (Figure 3 and 4). To our surprise, the sphericity of the catalysts is found to have insignificant effects on the attrition resistance. For the catalysts with precipitated silica (Figure 3), the catalysts are more spherical compared to the ones without precipitated silica (Figure 4), whereas the attrition resistances of the ones without precipitated silica are relatively better (Table 1). Further study of the catalyst structure at higher magnitude using SEM did not show any differences among the catalysts. Since iron oxide is the dominant phase in the particles, iron oxide crystals are the only elements observed.

Although the BET surface areas are found different for these catalysts, they do not appear to affect the attrition resistance of the catalysts. In general, the surface area increases with the increase in the support concentration for both series of catalysts. On the other hand, when plot the average pore size with the attrition resistance (weight loss of fines during jet cup tests), it appears for the series of catalyst without precipitated silica that the attrition resistance decrease with the increase of average pore size. On the contrary, the series of catalysts with precipitated silica, similar trend was not observed .

From the above analysis, it seems that the porosity of the catalyst particles appears to have some impact on the attrition resistance. Yet the mechanisms of the structure effects are not clear from the data above. It is known that the iron oxide itself does not have much attrition resistance, the supports incorporated in the catalyst particles obviously are the key elements in the attrition performance of the catalysts. It is therefore interesting to find out whether such structure of the supports also present in these iron catalysts and whether any egg-shell type structure of the supports also present in these iron catalysts and whether the formation of such structure is the key factor in the attrition resistance improvement as well.

Since the signals of iron oxide is much stronger than those of the silica supports during XRD and SEM measurements, the catalysts were therefore treated using HCl solution in order to resolve the iron oxide. The XRD results of some of the supports after acid leaching (Figure 5) show that the supports are all silica. The supports are also found not crystallized, which is considered to be due to the low calcination temperature of the catalysts.

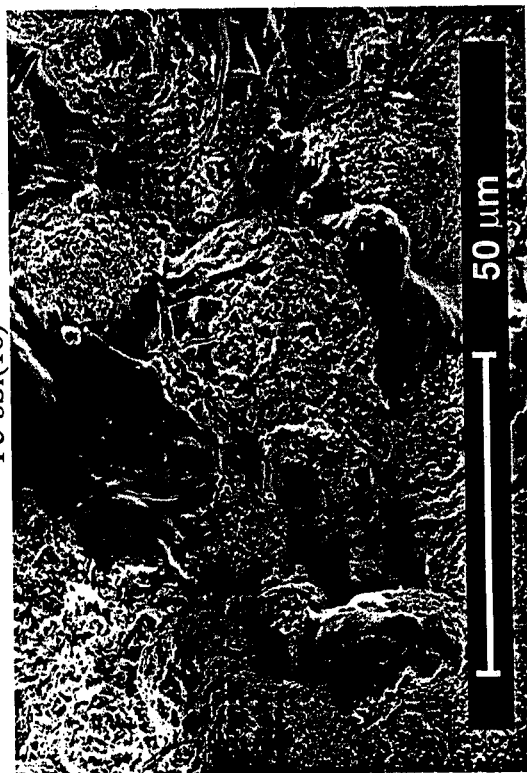
The study of the support morphology (Figure 6 and 7) shows that the supports for the catalysts appeared to be relatively smaller compared to the catalysts as prepared, especially for the catalysts without precipitated silica. The supports of the catalysts without precipitated silica appear to agglomerate more easily compared to those of catalysts with precipitated silica. When the supports were observed at higher magnification, it was found that these agglomerates were made of spherical particles (~30-40 μm in diameter) and some "amorphous" material (Figure 8). The XRD results (Figure 5) show that both of the spherical particles and the "amorphous" material should be silica, since no other elements present in the XRD patterns. It is, therefore, interesting to notice that silica exist in the catalyst particles seems to have two types: one forms the skeletal structure that appear to be spheres, the other appear to be more "amorphous" which causes agglomeration of the supports during drying.

For the supports of the catalysts with precipitated silica (Figure 9), the "amorphous" silica is seldom observed. Since the lacking of such "glue", these supports were not agglomerated much after the acid leaching. At higher magnification, it can be observed that the particles are spherical in shape and appear to be more porous (Figure 9) compared to the supports of the catalysts without precipitated silica (Figure 8). "Donut"-shape particles can also be found for the supports of catalysts with precipitated silica (Figure 6), whereas this type of particles is seldom observed for those of the catalysts without precipitated silica (Figure 7). It is

Figure 8. Morphology of the supports of the series of iron catalysts with binder silica at higher magnification
Fe-bSi(4)



Fe-bSi(16)



Fe-bSi(20)

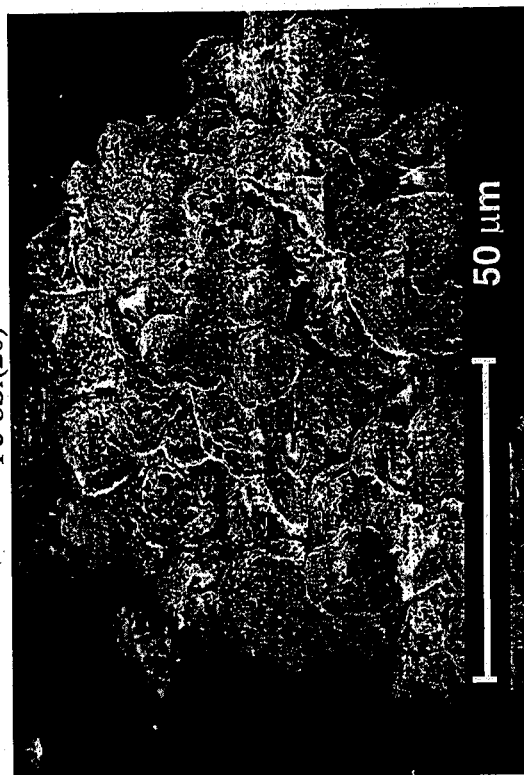
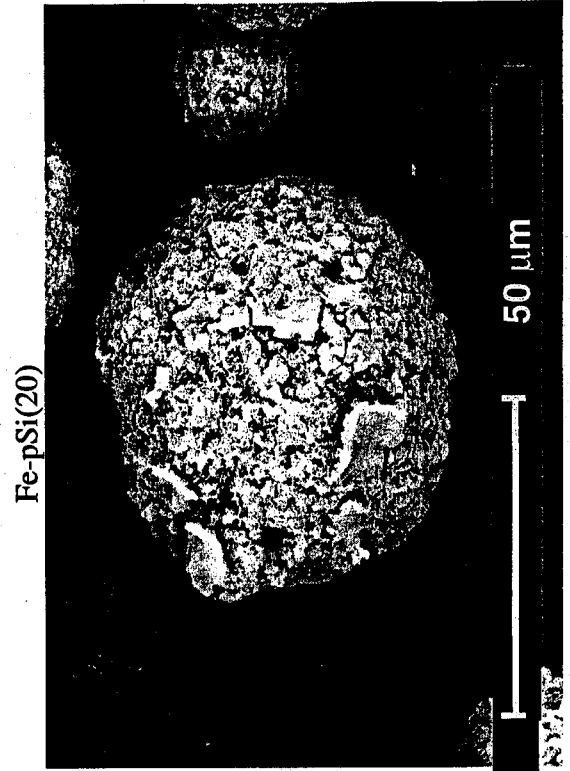
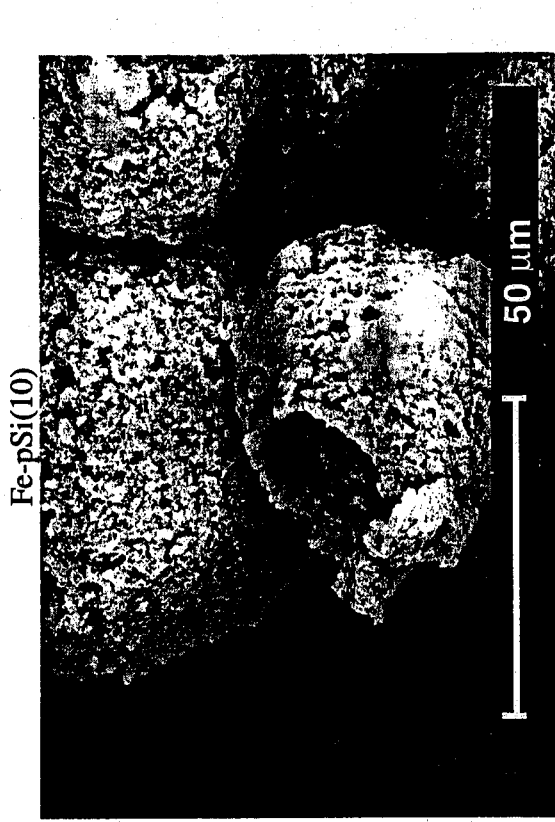
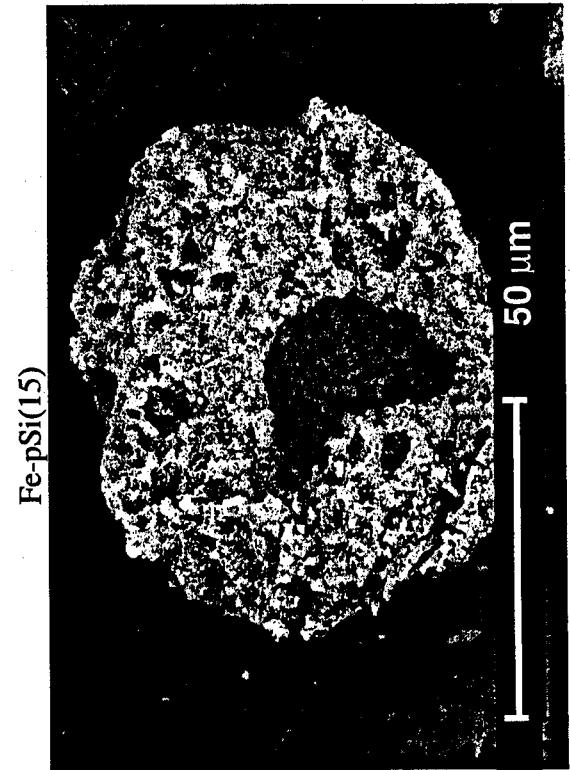
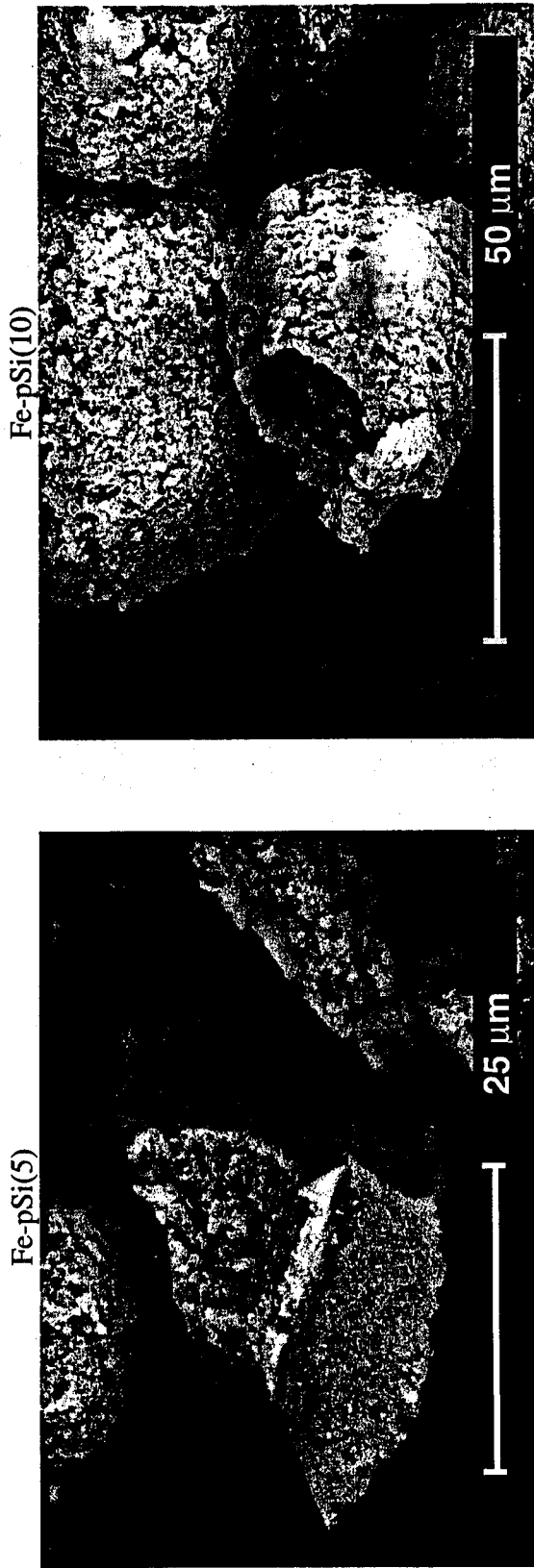


Figure 9. Morphology of the supports of the series of iron catalysts with precipitated silica at higher magnification



therefore speculated that addition of precipitated silica eliminated the existence of the "amorphous" silica and helped the silica to form a more porous structure. The increase in concentration of precipitated silica further increases the porosity of the supports. Such increase in the porosity of the supports is not beneficial for catalyst attrition resistance at all. On the contrary, decrease in the attrition resistance of the catalyst particle is observed with the increase of precipitated silica.

In Figure 9, a broken support particle of catalyst Fe-pSi(15) is shown. As can be seen, this particle is not only porous from an overall view, but also contains inner vacancy. Compared to a broken particle of the catalyst without precipitated silica (Figure 8), such porous structure is not observed. Instead, a much solid structure is found in Figure 8. These results are viewed as strong support of the above speculations. This also explains the "donut"-shape particles observed for the catalysts/supports with precipitated silica. Since the addition of precipitated silica facilitates the formation of a more porous structure and possible inner vacancies, such inner vacancy might be bigger enough that can be seen from outside the particles as a hole into the particle. In brief, it is suggested that the addition of the precipitated silica make it easy for the support to form primary silica particles and form more porous skeletal structure. It is also suggested to facilitate the formation of the structure with inner vacancy (shell type structure).

On the contrary, as seen in Figure 8, when precipitated silica is not added during catalyst preparation, the supports form less porous structure compared to those with precipitated silica. In addition, some silica seems to not form any primary silica particles (granules) but rather exist in an "amorphous" form. This less porous structure of the supports seems to provide better attrition resistance of the catalyst particle compared to the more porous structure of the supports. Another possibility is that the presence of the "amorphous" silica improved the attrition resistance. However, when the catalyst Fe-bSi(12) was studied, it is found that it is less likely

that "amorphous" silica is responsible for the catalyst attrition resistance improvement. Instead, for the support of the catalyst Fe-bSi(12), it is found that the support particles do not agglomerate as much as other supports for the same series of catalysts. A broken support particle of the Fe-bSi(12) catalyst (Figure 10) shows that this catalyst has a relatively more porous but uniform structure compared to other support particles of the same series of catalysts. No inner vacancy was observed for this catalyst even though it is porous. Other supports for the series of catalysts without precipitated silica, except for Fe-bSi(12), were found to have much less porous interior structure.

It is therefore speculated that at the absence of the precipitated silica, the support is less likely to form primary silica particle and therefore form less porous structure. The silica added seems to exist in the particle as an "amorphous" form. This more condensed structure (core type structure) seems to provide a better attrition resistance compared to the supports with shell type structures. However, there seems to be an optimum point between these two different types of structure. The catalyst of Fe-bSi(12) showed that when the porosity of the support is at a optimum point, where the inner vacancies are minimized, the porous structure became uniform through out the whole catalyst particles. At this point the presence of the "amorphous" silica is also eliminated to an amount that is not observable. The attrition resistance is the highest at this point.

Carburized Fe Catalyts

To further investigate the effects of phase change on catalyst attrition resistance, some of the spray dried catalysts were carburized under CO flow (Table 4). Surprisingly, the weight percentage of fines loss during jet cup test was found less compared to the attrition test of the same catalyst under calcined state.

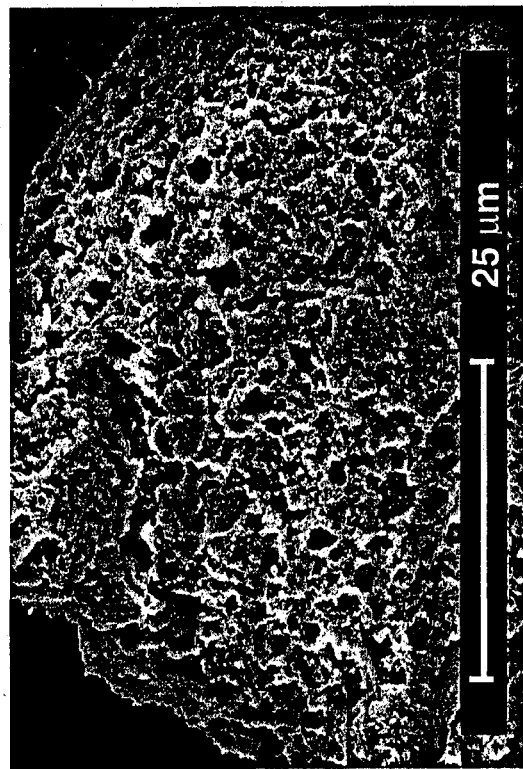
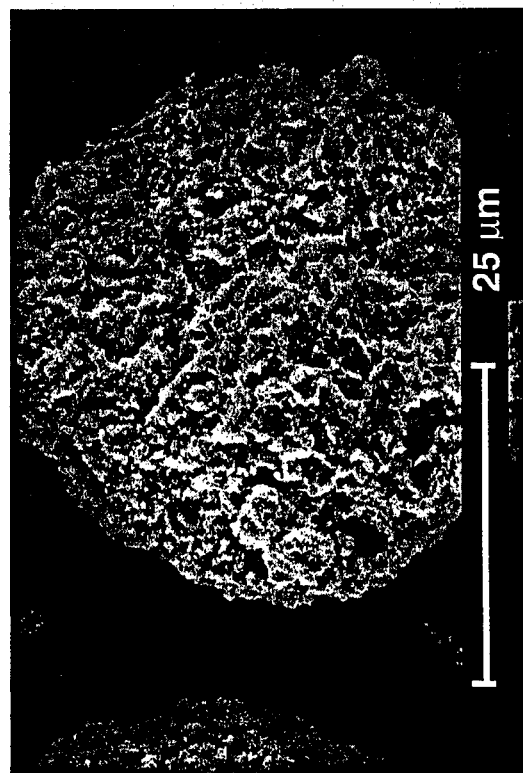
Table 4. Jet cup attrition resistance test results of the spray dried iron catalysts.

Catalyst	Coprecipitated Silica (pbw)	Binder Silica (wt%)	Fines (wt%) ^(a)		Bulk density (g/ml)	
			As received	After carburization	As received	After carburization
Fe/bSi(4)	0	4	26.6	--	0.83	--
Fe/bSi(8)	0	8	21.8	21.8	0.81	0.84
Fe/bSi(10)	0	10	4.8	7.7	1.02	1.08
Fe/bSi(12)	0	12	8.5	--	0.90	0.93
Fe/bSi(16)	0	16	18.2	15.5	0.78	1.18
Fe/bSi(20)	0	20	51.6	--	0.64	--
Fe/pSi(5)	5	12	26.6	13.2	0.66	1.09
Fe/pSi(10)	10	12	33.9	--	0.62	--
Fe/pSi(15)	15	12	39.6	--	0.61	--
Fe/pSi(20)	20	12	41.3	32.1	0.59	0.88
Co/SiO ₂ ^(b)	N/A	N/A	31.07	--	0.41	--

(e) Fines wt% = weight of fines collected/weight of total catalyst recovered

(f) Co/SiO₂ is a Davison 952 silica supported 20wt% cobalt catalyst, which was used for develop the procedure.

Figure 10. Morphology of the supports of the catalysts [Fe-bSi(12)] at higher magnification



6.0 CONCLUSION

Two series of spray dried iron catalysts were studied in the present research. Both of the series of catalyst were prepared similarly except for the difference in the concentration of the supports (precipitated and binder silica). It is found that the attrition resistances of these catalysts vary in a large range. The XRD results confirmed that all the catalysts after calcination are Fe_2O_3 in phase and similar in crystallinity. TPR results further show a unlike metal and support interaction. Physical properties was thereafter our research focus.

BET surface areas were found to increase with the increase in the concentration of the supports, but less relevant to the catalyst attrition resistance. On the other hand, average pore size of the catalysts seemed to have some impact on the attrition performance, but the effects are not clear from the porosity of the catalysts.

Since the iron oxide is known not to be attrition resistant, the catalysts were therefore treated using acid leaching in order to better study the support with a clearer vision. The XRD results of the supports showed that only silica remains after the acid leaching for all the catalysts. However, SEM micrographs of the support show that there seems to be two different types of silica existing in the catalysts. For the series of catalyst without precipitated silica, there are a type of "amorphous" silica in addition to another type of silica that forms spherical skeletal structure. Such spherical structure are, however, found to be smaller compared to the catalyst particles. This is considered to be a "core" type of structure. On the contrary, the addition of precipitated silica appears to eliminate the amount of such "amorphous" silica, and facilitate the formation of more porous skeletal structure, which even appears to contain inner vacancy. Such structure was found not beneficial for catalyst attrition resistance at all. It is also suggested that such "shell" type of structure is the reason of the formation of the so-called "donut"-shape

particles. With the increase in the concentration of precipitated silica, the skeletal structure of the supports becomes more porous and therefore less attrition resistant.

For the series of catalysts without precipitated silica, it is found that the presence of such "amorphous" silica does not improve the attrition resistance of the catalysts. On the other hand, it is the less porous structure appear to be more attrition resistant compared to the more porous structure of the series of catalysts with precipitated silica. However, such "core" type of structure does not seem to provide the best attrition resistance either. It is found that only when the skeletal structure is porous and uniform can the catalyst particles have the best attrition performance.

Since phase change during reaction has always been a concern for iron catalysts in terms of attrition resistance, some of the catalysts were carburized and tested using the jet cup. The attrition resistance was found to actually improve after carburization in terms of weight percentage of fines lost. Such improvement was considered to be due to the change in catalyst bulk density upon carburization.

7.0 References

- Allen T., in "Particle Size Measurement, 5th ed.", Chapman & Hall, New York, 1997, p.45.
- Bhatt, B.L., Heydorn, E.C., and Tijm, P.J.A., in "Proceedings of the 1997 Coal Liquefaction & Solid Fuels Contractors Review Conference", US Department of Energy, Federal Energy Technology Center, Pittsburg, Pennsylvania, 3-4 September, 1997, p. 41.
- Bukur D.B., Nowicki L., and Patel S., *Can. J. of Chem. Eng.*, 74 (1996) 399.
- Bukur D.B. Patel S.A., and Lang X., *App. Catal. A*, 61 (1990) 329.
- Huang, C-S, Xu, L., and Davis B.H., *Fuel Sci. Tech. Int'l.*, 11 (1993) 639.
- Jothimurugesan, K., Goodwin, J.G., Jr., Spivey, J.J., and Gangwal, S.K., *Syngas Conversion to Fuels and Chemicals*, American Chemical Society, 1999.
- Kalakkad, D.S., Shroff, M.D., Kohler, S., Jackson N., and Datye, A.K, *App. Catal. A*, 133 (1995) 335.
- Schulz, *Nat. Gas Conv. II, Surf. Sci. Sci. Ser.*, vol. 81, Elsevier, New York, 1994, P.455.
- Srinivasan, R., Xu, L., Spicer, R., Tungate, F.L., and Davis B.H., *Fuel Sci. Tech. Int'l.*, 14 (1996) 1337.
- Zhao, R., Goodwin, J.G., Jr., and Oukaci, R., *App. Catal. A*, in press (1999)